JURNAL SAINS MATERI INDONESIA (JUSAMI)
ISSN: 1411-1098 (print), 2614-087X (online)
VOL. 25, ISSUE 1, 2023
DOI: 10.55981/jsmi.267

ORIGINAL ARTICLE

Effect of 2-Methylimidazole Composition as Low-Temperature Application in Phenol-Formaldehyde, Glycidyl Ether Epoxy Coating

R. F. Paltgor[1], R. Riastuti[1], R. T. Ramdhani[1], M. Yunus[2]

[1]Faculty of Engineering, Universitas Indonesia, Indonesia
[2]Research Center for Polymer Technology, National Research and Innovation Agency, Indonesia

ABSTRACT – The addition of materials to pile pipe at low temperatures is very challenging. Thereby, an optimum operating level is needed to produce a quality coating. Furthermore, 2-methylimidazole (2MI) was added into a phenol-formaldehyde, glycidyl ether polymer fusion bonded epoxy (FBE) coating at different concentrations of 1, 2, and 3 %wt. Thermal analysis was then carried out using differential scanning calorimetry (DSC), where the addition of 2MI decreased the curing temperature to 134.76°C due to the reduced activation energy. Potentiodynamic polarization showed the best corrosion rate of 0.00991 mm/year with a current density of 0.847μA/cm^2 after adding 1 %wt 2MI. Electrochemical impedance spectroscopy (EIS) was carried out to determine the charge transfer resistance and maximum coating capacitor capacitance after adding 1 %wt 2MI, namely 9.9 kΩ and 8.45×10-5 F, respectively. The cathodic disbondment test (CD-Test) showed that the disbondment radius of the coating under the influence of the cathodic protection current was 4.32mm. Mechanical analysis by pull-off adhesion test showed a value of 7.28 MPa after the addition of 2MI 2 %wt but decreased to 6.63 MPa at 3 %wt. Therefore, the optimum addition is 1 %wt 2MI for low-temperature applications of 170 –175°C in piles with high coating performance and compliance with predetermined standards.

ARTICLE HISTORY
Received: 6 February 2023
Revised: 16 June 2023
Accepted: 2 August 2023

KEYWORDS
2-Methylimidazole
Coating performance
Low temperature
Pile pipe

INTRODUCTION

Carbon steel is still widely used as a basic material for producing pipes because it has good mechanical properties, is easy to fabricate, and has a low cost compared to expensive stainless steel [1]. However, one of its major weaknesses is the low resistance to corrosion compared to stainless steel [1]. In the industrial era, fusion bonded epoxy (FBE) was used in the oil and gas industry, such as Bronang Gas and Mebidang Kota project. Several construction fields have used pipe piles with FBE coating to prevent corrosion. The performance of this coating is very challenging due to its high cross-linking density. The curing agent affects the reactivity of epoxy resins and determines the type of chemical bond and the level of cross-links formed [2]. In the epoxy powder application process, liquid FBE flows on the surface treated with sandblasting and acid washing. The hydroxyl groups then react with the molecular chains to form a very strong coating layer. The polymer chain must be able to carry out adequate cross-linking reactions in the film profile to minimize internal stress [3]. The resin molecule in FBE contains three rings of oxirane, which are very reactive during curing at high temperatures of 180^{o}C to 200^{o}C for low-temperature applications (low application temperature). The curing temperature can reach 250^{o}C with high FBE temperature glass (T_g) [4]. Furthermore, the coating does not require solvents to keep the binder and filler in liquid form during the application process. A non-crystalline solid is often formed by maintaining the glassy properties of the polymer at an operating temperature of 65^{o}C. Modification of the FBE (brominated phenyl functional group) molecule chain can increase the T_g, thereby leading to increased adhesion and resistance to cathodic disbondment in coatings [4]. The dispersion of materials, such as carbon black as a filler in the powder, has been reported to have the ability to reduce the porosity and movement of the chain segments [5]. However, the addition of a large amount of filler can increase the tendency of agglomeration formation, reducing its protective ability. This indicates that the shape and size of the filler play an important role in erosion resistance [6]. In the development era, FBE is often applied in several fields besides the oil and gas industry. Several construction sectors have used pipe piles with FBE coating to prevent corrosion. The X manufacturers can only perform optimal coating on a maximum pipe diameter of 32 inches. To carry out coating with a diameter of more than 40 inches, such as those used for pile pipes based on customer specification, a greater energy level is required to achieve the optimum application temperatures. The addition of 2-methyl imidazole (2MI) has been reported to greatly reduce the curing reaction temperature as well as improve the mechanical and thermal properties of the mixture. This is because 2MI is more active in initiating the cross-linking process quickly [7]. It is also more effective compared to 1-methylimidazole, 2-ethylimidazole, 2-phenimimidazole, 2-ethyl-4(5)-methylimidazole 1-(2-cyanoethyl)-2-ethyl-4(5)-methylimidazole in initiating the polymerization of epoxy resins [8],[9]. Jie Xu et al. earlier reported that 2MI in the E-20/HMTA systems could decrease the activation energy and increase the rate of curing reaction [10]. The addition of 2-methylimidazole as a curing agent can accelerate the curing process and reduce the application temperature required in the process of coating on large-diameter pipes. Therefore, this study aims to obtain the optimum coating results for coating pipes with diameters > 40 inches based on predetermined standards.

***CORRESPONDING AUTHOR** | R.F. Paltgor | ✉ rinush.fedrikdo@ui.ac.id

EXPERIMENTAL METHOD

Materials and Instruments

2-methylimidazole (2MI) as a curing agent and epoxy phenol-formaldehyde, glycidyl ether polymer was supplied by Jotun Powder Coating Indonesia. The test material used in this study included API 5L PSL 2 pipe with grade L360MO/X52MO.

The equipment used in this paper are differential scanning calorimetry (DSC) Q20 TA instrument for thermal analysis, Bruker Tensor 27 Fourier transform infrared (FTIR) for chemical structure analysis, Corrtest Instrument for electrochemical impedance spectroscopy (EIS) and potentiodynamic polarization.

Method and Procedure

In this study, 2-methylimidazole (2MI) was added to a mixture of epoxy phenol-formaldehyde, glycidyl ether polymer in a fluidized bed. Furthermore, its application was carried out using the electrostatic spray method with a composition of 1, 2, and 3 weight percent (%wt) 2-methylimidazole to reach a thickness of 300 µm each specimen. Surface preparation was carried out using the blasting method. The test material used in this study included API 5L PSL 2 pipe with grade L360MO / X52MO.

Thermal characteristics were carried out using differential scanning calorimetry (DSC) of 2-methylimidazole in a mixture of epoxy phenol-formaldehyde, glycidyl powder ether [11]. Characterization was then performed using DSC with the Q20 TA Instrument.

After the thermal analysis, the mixed powder was applied to pipes at a temperature range of 170–175ºC. Furthermore, to determine the performance of fusion bonded epoxy (FBE), a ring test sample was taken by cutting a pipe coated with FBE with a size of 100mm × 100mm × thickness.

FTIR spectra are often used to determine changes in the chemical structure of an organic compound. The coating layer in this study was analyzed using a Bruker Tensor 27 at room temperature with wavelengths of 4000 to 500 cm^{-1}.

The cathodic protection resistance was determined using the cathodic disbondment test with the Canadian standard CSA Z245-20 method in 3 %wt NaCl solution at 65ºC for 24 hours [12]. The corrosion rate was then assessed with potentiodynamic polarization and electrochemical impedance spectroscopy (EIS) methods based on ISO 17463, with a range of 0.01–105 Hz [13].

The mechanical characteristics were determined using the adhesion strength test by evaluating the pull-off adhesion based on American Standard Testing and Material (ASTM) D4541 [14]. Furthermore, visual observation of the cross-section of the layer and its morphology was carried out to assess the porosity level of the FBE [11].

RESULT AND DISCUSSION

Thermal Characterization

Differential Scanning Calorimetry (DSC) Testing

Thermal characterization was performed after mixing the fusion bonded epoxy (FBE) material and 2-methylimidazole (2MI) powder. The characterization was performed to determine the effect of adding 2-methylimidazole on the behavior of the powder during the heating process. Furthermore, an analysis of each 2-methylimidazole composition was also carried out in this study. Several points can be considered from this thermal analysis, namely the glass temperature (T_g), curing onset temperature (T_{onset}), curing end set temperature (T_{endset}), and enthalpy energy (ΔH) required during curing. The heating process was carried out to a temperature of 250ºC with an increase rate of 20ºC/min. The results of the data on the powder are presented in Figure 1 and Table 1 below.

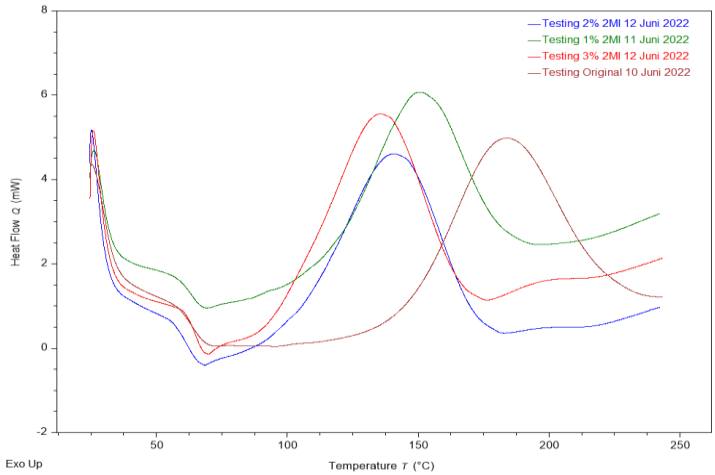

Figure 1. DSC curves of FBE with addition 1, 2, and 3 %wt 2MI

Table 1. Results of powder DSC testing

Specimen	T_g (ºC)	T_{onset} (ºC)	T_{peak} (ºC)	T_{endset} (ºC)	ΔH (J/g)
FBE	64,15	109,71	182,90	243,26	62,94
FBE, 1 %wt *2MI*	63,91	84,06	150,48	213,48	54,24
FBE, 2 %wt *2MI*	61,34	52,31	140,64	184,28	52,31
FBE, 3 %wt *2MI*	60,74	83,17	134,76	179,87	60,51

Based on the differential scanning calorimetry (DSC) curve for the specimen, all powders have the same thermal characteristics, where they experience a glass transition at a temperature of 60–65ºC. This was because the imidazole group does not have substitutional functional groups [8]. Furthermore, the powder began to experience a cross-linking polymerization reaction at 180–250ºC due to further heating. The process was marked by the formation of a peak curve, which indicated that the reaction was exothermic. This finding showed the behavior of thermosetting materials, which often react at high temperatures. The addition of 2MI caused a shift in the polymerization reaction process towards low temperatures. The maximum results were obtained from the use of 3 %wt 2MI, which reduced the values from 64.15ºC to 60.74ºC when starting the curing process, 182.90°C to 134.76°C for the peak curing temperature process, and 243.26°C to 179.87°C at the and end of the curing reaction, respectively. The results also showed that it caused a 4°C decrease in the glass temperature of FBE, which is expected to speed up the process.

The addition of 3 %wt 2MI was the best choice when using FBE in low-temperature applications because the lowest peak temperature was 134.76ºC. The results showed that using 2MI can accelerate the polymer reaction with epoxy [8]. Jie Xu [10] stated that the addition of the additive 2MI in Bisphenol A epoxy resin (E-20) reduced the activation energy and increased the curing reaction rate.

This study showed that the application of 2MI reduced the exothermic energy during the polymerization process. However, at a concentration of 3 %wt, the required energy increased because it released a large amount of energy to complete the curing process. The results also showed that it led to the production of additional imidazole-epoxy products and reduced the anionic polymerization reaction [8]. Further analysis was carried out after the thermal characterization of the analytical powder was determined during the curing process. The curves and results of thermal analysis on dry FBE are presented in Figure 2 and Table 2 below.

Table 2. Glass temperature of fusion bonded epoxy

Specimen	T_g (ºC)
FBE	113,51
FBE, 1 %wt *2-methylimidazole*	108,80
FBE, 2 %wt *2-methylimidazole*	105,31
FBE, 3 %wt *2-methylimidazole*	102,50

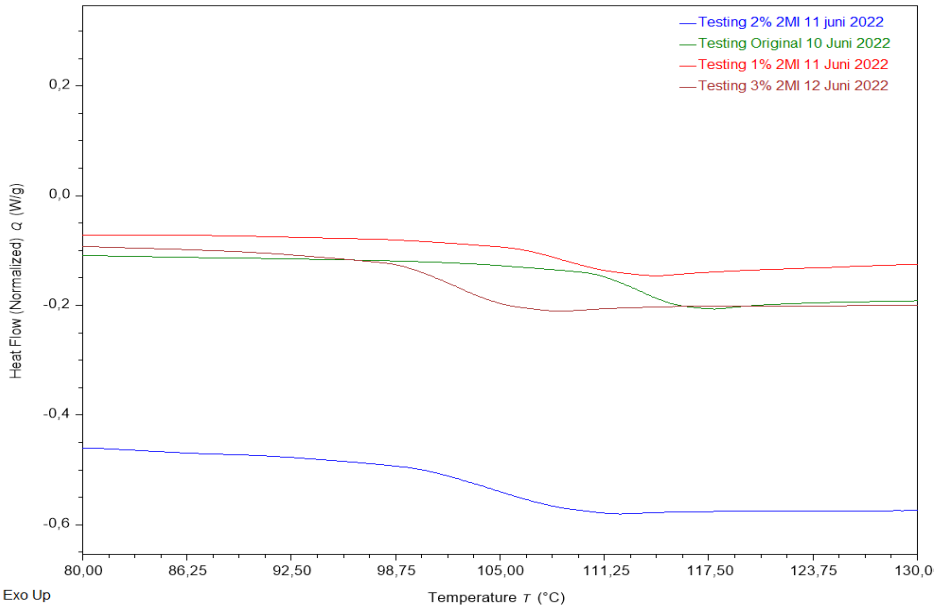

Figure 2. DSC curve of cured fusion bonded epoxy

Figure 2 shows that the addition of 2MI produced glass temperatures within the range of 102 –114ºC. The glass temperature change indicated that the powder material had decreased the curing process temperature. Furthermore, the lowest value was obtained using 3 %wt 2MI with 102.5ºC. The initial glass temperature of FBE was 113.51ºC but

decreased to 108.80°C along with a shift in the curve after adding 1 %wt of the sample. The addition of 2 %wt 2MI lowered the value obtained to 105.31ºC. The results showed that the highest decrease to 102.5° occurred at a concentration of 3 %wt. The addition of 3 %wt 2MI showed a significant difference compared to other samples. The incorporation of 2-MI could decrease the activation energy and increase the rate of transition reaction. During the glass phase change reaction process, the heat flow in addition 2 %wt 2MI was very low, namely -0.45 to -0.6 W/g. This is due to the impurities that affect the heat flow during phase change reactions that need more energy, where segments in the chains were moving not in a cooperative manner. For samples 0, 1, and 3 wt% 2MI, the glass phase change was observed with a heat flow of -0.06 to 0.2 W/g.

Chemical Structure Characterization with Fourier Transform Infrared (FTIR)

FTIR was carried out to determine changes in the chemical structure of the FBE layer after adding 1, 2, and 3 %wt 2MI with a wavelength of 4000 to 500 cm^{-1}. The results of the FTIR test on the four samples were presented in the form of a curve, as shown in Figure 3.

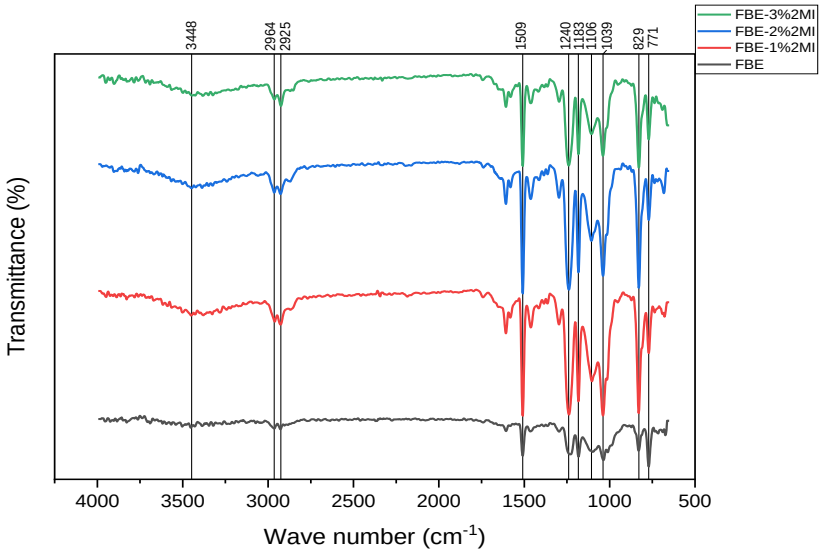

Figure 3. Infrared Fourier transform curve on FBE and each addition of 1, 2, and 3 %wt 2MI into FBE

Figure 3 shows that several peaks were formed in the coating at 771 and 829 $cm^{-1,}$ where bending vibrations of the C-N functional group were observed [15]. At 1039 and 1183 cm^{-1}, the functional group stretching vibrations of the ether group were formed. Furthermore, the 1509 cm^{-1} peak was the functional group of the N-H bond. The peak at 2925 cm^{-1} and 2964 cm^{-1} were the stretching vibrations of the functional group from methylene C-H and methyl C-H, respectively [16]. The last peak at 3448 cm^{-1} was the functional group of the –OH structure and was associated with the strongest hydroxyl bond interaction in the phenol group [17]. The absorption peaks of the C-N functional group band at 771 and 829 cm^{-1} increased. These results indicated that the successful amine in the imidazole was added to the epoxy group to form cross-linked polymers.

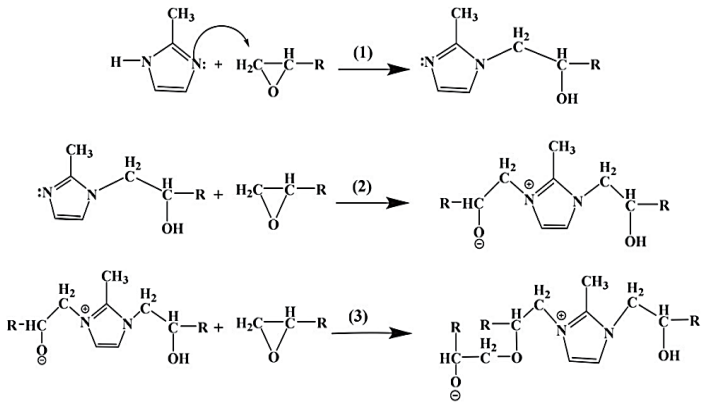

Figure 4. Curing reaction of 2MI in FBE

After the addition of 2MI as an anionic polymer into the FBE, the curing reaction occurred in 2 stages. The active hydrogen of the secondary amine in the imidazole was added to the epoxy group, and intramolecular complexes of positive and negative ions were formed by generating adducts and other epoxy groups. Negative ions in the center of the complex, which can catalyze the epoxy ring opening reaction and finally react with curing agents and other epoxy groups [18], are shown in Figure 4. However, after adding more than 1 %wt 2MI, there was a decrease in peak absorption in the

coating. This indicated a reduced reaction density, which was elicited by 2MI as a catalyst, as well as an increase in the cross-linking polymerization reaction rate on the epoxy during the curing process.

Electrochemical Characterization

Cyclic Potentiodynamic Polarization (CPP)

CPP was carried out to obtain the potential values of pitting corrosion (E_{pit}), repassivation potential (E_{rep}), corrosion potential (E_{corr}), corrosion current density (I_{corr}), and corrosion rate. Furthermore, Figure 5 shows the CPP yield curve for each specimen. From the CPP yield curve, corrosion potential (E_{corr}) and corrosion current density (I_{corr}) were obtained, as shown in Table 3. The potential value was measured using the saturated calomel electrode (SCE) reference electrode in a 3.5% NaCl electrolyte solution.

The results of electrochemical characteristics with potentiodynamic polarization, which produced anodic and cathodic polarization curves, are presented in Figure 5:

$$\text{Anodic: } Fe_{(s)} \rightarrow Fe^{2+}{}_{(aq)} + 2e^- \quad (1)$$

$$\text{Cathodic: } 2H_2O_{(aq)} + 2e^- \rightarrow H_{2(g)} + 2OH_{(aq)} \quad (2)$$

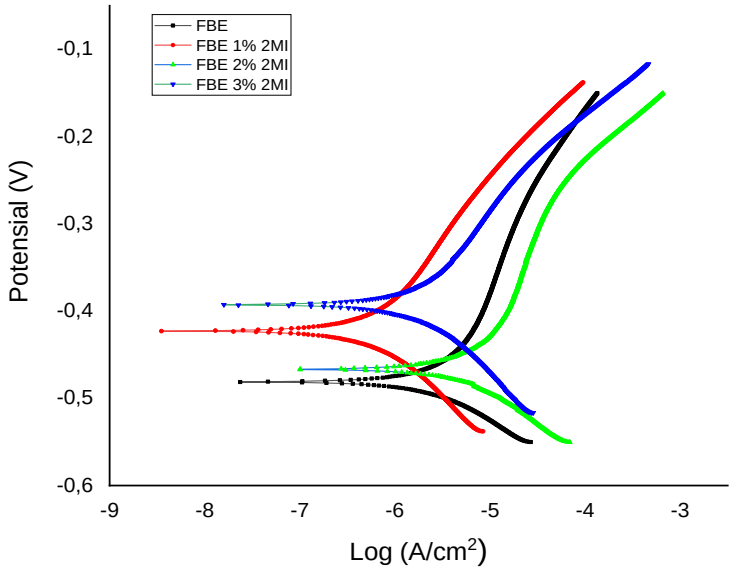

Figure 5. Tafel curve of CPP each specimen

Figure 5 shows the addition of 2MI in FBE. Corrosion potential (E_{corr}) value increased from -0.48126V to -0.46684V, -0.42286V, and -0.39282V at 2, 1, and 3 %wt 2MI, respectively. 2MI, as a curing agent, caused a shift in the polarization curve towards the anodic region (positive), which indicate that the addition of 2MI can improve corrosion resistance. Table 3 shows that the initial current density of the FBE was 5.32µA/cm^2, but the value decreased after the use of 2MI. Furthermore, the greater the value obtained, the easier it is for the charge to diffuse in the coating structure, and this causes an increase in the corrosion rate. The maximum current density value was reduced after the addition of 1 %wt 2MI to 0.84 µA/cm^2. According to Figure 5, adding 1 %wt 2 MI will indent the curve to the left before adding the addition. After adding more 2MI, the current density in the FBE was later increased, according to the polarization curve, where the curve shifts to the right. This was due to changes in the molecular structure in the coating as well as the reduced cross-linking density [10].

Table 3. The results of measurements of corrosion potential and corrosion current density in all specimens

Specimen	E_{corr} (V)	I_{corr} (A/cm^2)	CR (mm/year)
FBE	-0,48126	$5{,}3225 \times 10^{-6}$	0,06227
FBE, 1 %wt 2MI	-0,42286	$8{,}4703 \times 10^{-7}$	0,00991
FBE, 2 %wt 2MI	-0,46684	$1{,}2086 \times 10^{-5}$	0,14139
FBE, 3 %wt 2MI	-0,39282	$2{,}3874 \times 10^{-6}$	0,02793

The corrosion rate (CR) that occurred in the coating can be determined based on the current density values. Furthermore, the value of the corrosion rate can be obtained using the equation below.

$$CR = \frac{3{,}27 \times 10^{-3}\ a\ icorr}{n\ D} \quad (3)$$

Where the density of the substrate (D), namely iron, was 7.87 g/cm^3, the weight equivalent of an iron atom that undergoes oxidation (a) was 2 × 27.92. The number of electrons that experienced exchange (n) was 2. Hence, the CR value (mm/year) in each sample can be determined, as shown in Table 3.

After calculating the corrosion rate, the value obtained was directly proportional to the current density. Besides reducing the curing temperature, 2MI can also lower the corrosion rate. The best result was obtained from the addition of 1 %wt 2MI, where the value obtained was 0.00991 mm/year, compared to the sample without the treatment, namely 0.06227 mm/year.

Electrochemical Impedance Spectroscopy (EIS) Testing

EIS was performed to characterize the coating on the steel pipe surface due to interaction with the environment or the electrolyte solution. The electrochemical properties of the specimen equivalent circuit were also determined from the EIS testing using the ZSimpWin 3.21 software. Furthermore, EIS was carried out using SCE, graphite rod, and the specimen as the reference, opposing or complementary, and working electrode in 3.5% NaCl electrolyte solution, respectively. The frequency used in this study was 10,000 Hz to 10 Hz within 5 minutes.

Figure 6 shows the Nyquist plot of all samples subjected to the EIS test at 5 minutes. Based on the results, the Nyquist plot in the samples has a different semicircle profile size, indicating that each sample has a different resistance value. Furthermore, this semi-circular curve represents the transfer resistance value (R_{ct}). The larger the diameter of the curve, the greater the value of the charge transfer resistance (R_{ct}) of the coating and the lower the corrosion rate on the substrate. Adding 1 %wt will increase the size of the semicircle profile before addition. Where Z_{real} reaches a value of 1.0 E + 10 and $Z_{imaginer}$ reaches 5E + 09. However, after further addition, the semicircle profile size will decrease. This shows that adding 1 %wt 2MI will reduce the resistance value of the coating, which will result in reduced corrosion resistance of the coating and coating performance. The resistance values obtained in this study are presented in Table 4 below.

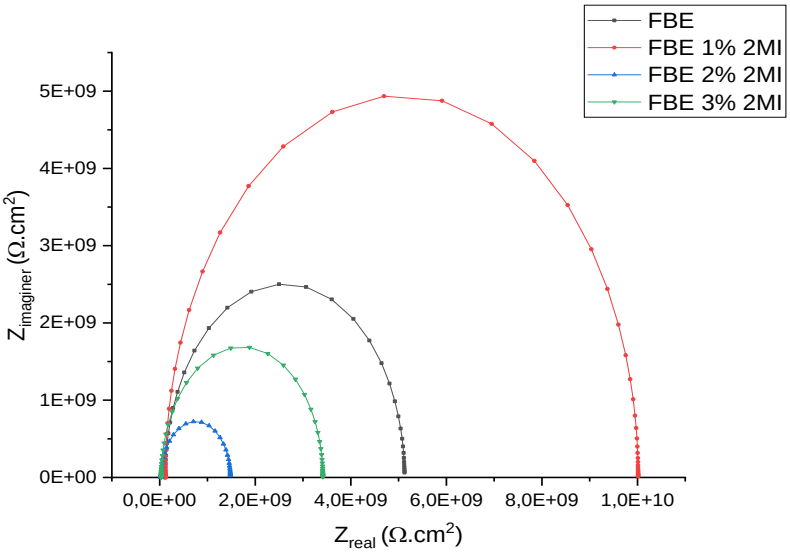

Figure 6. Nyquist plots each specimen

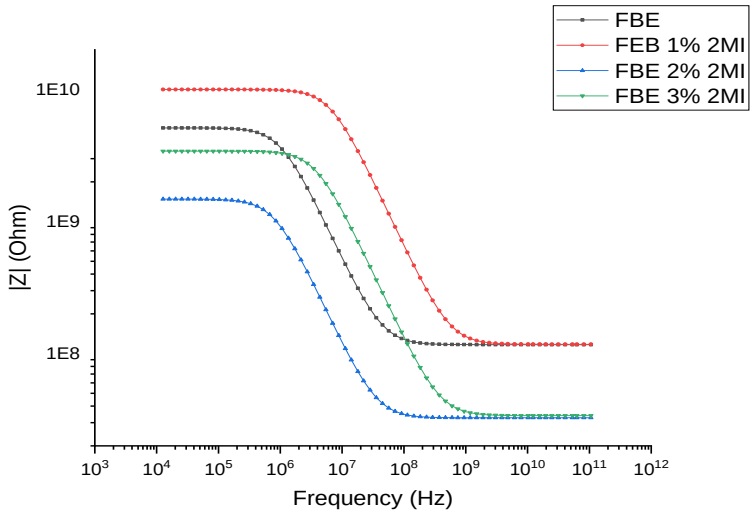

Figure 7. Bode plot of each specimen

Figure 7 shows the resistance to the flow of charge on the sample in terms of frequency. The use of 1 %wt 2MI caused an increase in the resistance of FBE, but further addition lowered the value. This was due to changes in reaction

during the curing process, polymerization only occurred with anionic reactions. However, there was an additional epoxy-imidazole product reaction in FBE, which accelerated the process and changed the cross-linking structure. The reduction in cross-linking reaction density from anionic polymerization can reduce the ability of the coating to lower the corrosion rate in salt solutions. This decreased density made it easier for the charge to diffuse through the coating. Equivalent circuit modeling was also done to obtain electrochemical properties, such as resistance, capacitance, and constant phase element (CPE).

Table 4. Fitting results of EIS testing

No	Specimen	Equivalent Circuit	R_s (Ω)	R_{ct} (Ω)	C (F)	CPE (F)	N
0	FBE	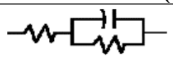	5.9	5008	3.12E-05	N/A	N/A
		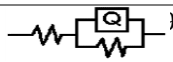	0.3	3.78E+04	N/A	4.02E-04	0.4344
1	FBE, 1 %wt 2MI	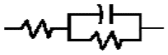	7.5	9902	2.46E-06	N/A	N/A
		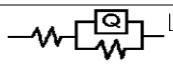	1.16	20000	N/A	8.48E-05	0.4819
2	FBE, 2 %wt 2MI	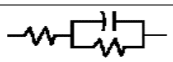	67	1448	1.38E-04	N/A	N/A
		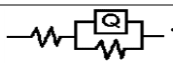	.49	3172	N/A	1.15E-03	0.5142
3	FBE, 3 %wt 2MI	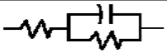	87	3382	1.24E-05	N/A	N/A
		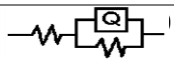		7944	N/A	3.36E-04	0.4974

The value of the charge transfer resistance of each coating varied based on the type of coating. A high transfer charge resistance (R_{ct}) represents a low corrosion rate due to the presence of a coating layer that protects the metal surface from direct contact with the electrolyte [19].

Based on Table 4, the initial load transfer resistance value was 5008 Ω. After the addition of 1 %wt 2MI will increase transfer resistance to 9902 Ω, indicating that 2MI will increase the density of the material. But, the value was reduced after adding more 2MI sequentially, namely 1448 Ω and 3382 Ω. The addition of more than 1 %wt 2MI made a reduction in cross-linking reaction density from anionic polymerization and reduced the ability of the coating with a higher corrosion rate in salt solutions. This decreased density made it easier for the charge to diffuse through the coating. This indicated that the addition of 1 %wt 2MI can produce excellent charge transfer resistance in resisting the corrosion rate from the aggressive attack of 3.5% NaCl solution.

Furthermore, there are other electrical elements, namely double-layer capacitance (Cdl) elements, which represent the double-layer capacitance values of electrical equivalent circuit fittings. A constant phase element with a value of N = 1 acts as a pure capacitor. A CPE is often used as a double-layer capacitance (Cdl) model to compensate for surface inhomogeneity. This was caused by rough and porous metal surfaces, defects, and other interface phenomena. The smaller the double-layer capacitance (Cdl) value, the higher the thickness. This can cause a decrease in the corrosion rate due to the adsorption of coating molecules on the metal surface, thereby preventing direct contact with aggressive solution molecules [20]. The results showed that the four specimens had very low CPE values within the range of 1.15E-03 F to 8.48E-05 F.

Cathodic Disbondment Testing

Resistance of the coating to cathodic protection currents was tested using the cathodic disbondment test. A hole (holiday) of 3.3mm was given in the middle of the sample, and it penetrated the substrate. The test was carried out in 3.5 % NaCl solution at 65°C, and the sample was then given a voltage of 3.5 V for 24 hours. An evaluation was carried out by peeling at the eight angles from the direction of the hole towards the FBE layer. The results of the cathodic disbondment test are presented in Figure 8.

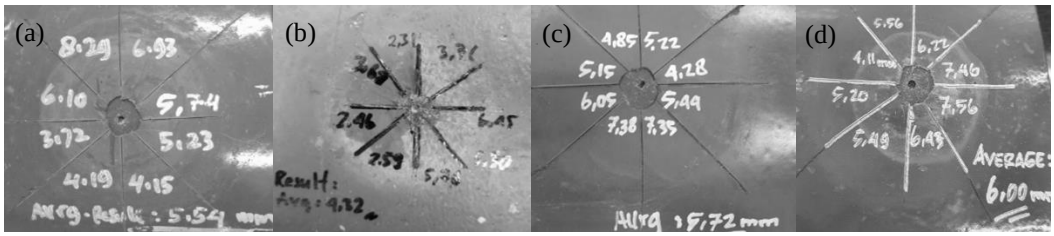

Figure 8 Cathodic disbondment test results on (a) FBE, (b) FBE 1 %wt 2MI, (c) FBE 2 %wt 2MI, and (d) FBE 3 %wt 2MI

Based on the results, increasing the composition of 2MI reduced the resistance of the FBE to cathodic currents. Furthermore, the smallest resistance occurred in the 3 wt% composition, which can reach 6mm/day. The addition of 2 %wt and 1 %wt produced values of 5.72 mm/day and 5.54 mm/day, respectively. This finding shows the resistance of the coating to concentrated cathodic polarization attack without the addition of 2MI, namely 4.32 mm/day.

This is in line with the results of the bode plot analysis, where the resistance value in the sample decreased with an increase in the composition of 2MI. A reduced value can speed up the process of charge diffusion in the coating hole. Min Xu et al. [21] revealed that the reactions that occurred during the cathodic reaction consisted of the following:

$$2H_2O + 2e^- \rightarrow 2OH^- + H_2 \quad (4)$$

$$O_2 + 2H_2O + 4e^- \rightarrow 4OH^- \quad (5)$$

Based on the results of the corrosion during the process of giving a cathodic current, a white product was obtained due to the dissolution of the iron oxide layer. The failure mechanism of cathodic peeling was caused by the dissolving of the oxide layer, which can damage the mechanical bond between the coating and the steel surface. Furthermore, the increasing pH level in the solution led to a local attack on the coating through saponification or hydrolysis [22].

The reaction of dissolution/reduction of iron oxide:

$$Fe_2O_3 + 3H_2O + 2e^- \rightarrow 2Fe(OH)_2 + 2OH^- \quad (6)$$

$$2H_2O + 2e^- \rightarrow 2OH^- + H_2 \quad (7)$$

The oxygen reduction reaction damaged the coating:

$$O_2 + 2H_2O + 4e^- \rightarrow 4OH^- \quad (8)$$

Equation (8) shows that the oxygenated solutions can bring the reaction from concentration to activation polarization. This is expected to cause a higher number of hydroxyl ions around the holiday, thereby leading to greater disbondment [21]. Furthermore, the transfer of a layer with a high pH film, which can be formed by diffusion of water and electrolyte ions to the substrate interface, initiated the disbondment process. Oxide dissolution was caused by exposure to high-alkaline media after exfoliation [23].

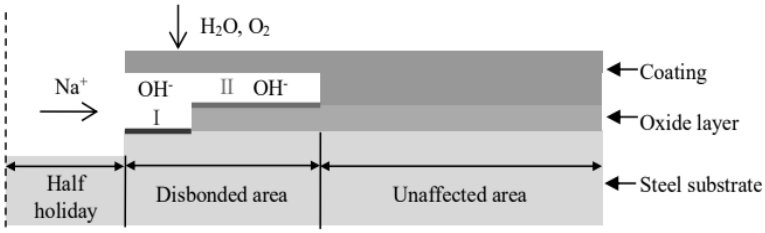

Figure 9. Schematic of coating disbondment due to the dissolution of the oxide layer

Mechanical Characterization

Adhesion Testing

In mechanical characterization, the adhesion strength was determined using the adhesion pull-off test (adhesion pull-off test) with 4-panel samples measuring 250mm × 250mm. The test was carried out by attaching a 20mm dolly using adhesive glue to ensure that it adhered to the surface of the specimen coated with scoring before testing was carried out. Furthermore, the test was performed after the coating had experienced a perfect ripening process, and the results are presented in Figure 10 and Table 5 below.

Based on the results, sample 0 has a pull-off strength value of 5 MPa, where the first, second, and third points were 4.64 MPa, 5.52 MPa, and 4.84 MPa, respectively. For the nature of the fracture, a visual inspection is carried out to determine the fracture's surface and assesses the type of fracture based on ISO 4624. Figure 10 (a) shows that 50% fracture occurred in the FBE cohesive and between the FBE and glue adhesive. In sample 1, the addition of 1 %wt 2MI caused an increase in the pull-off adhesion strength value to 5.3 Mpa, where the first, second, and third points were 5.07 MPa, 5.56 MPa, and 5.27 MPa, respectively.

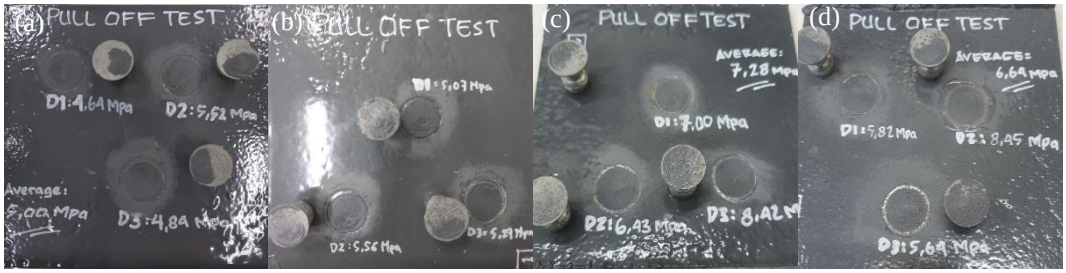

Figure 10. Pull-off adhesion test results on (a) FBE,

(b) FBE 1 %wt 2MI, (c) FBE 2 %wt 2MI, and (d) FBE 3 %wt 2MI

Table 5. Pull-off adhesion results

No	Specimen	Result			
		X1 (Mpa)	X2 (Mpa)	X3 (Mpa)	Average (Mpa)
0	FBE	4,64	5,52	4,84	5,00
1	FBE, 1 %wt 2MI	5,07	5,56	5,27	5,30
2	FBE, 2 %wt 2MI	7,00	6,43	8,42	7,28
3	FBE, 3 %wt 2MI	5,82	8,45	5,64	6,63

Figure 10 (b) shows that fracture occurred in 60% of the FBE cohesive, and 40% was observed in the glue adhesive. Furthermore, the addition of 2 %wt 2MI was carried out for sample 2, where the pull-off adhesion strength experienced a peak increase of 7.28 MPa, where the first, second, and third points were 7.00 Mpa, 6.43 Mpa, and 8.42 Mpa, respectively. Based on Figure 10(c), fracture occurred in 70% of cohesive FBE, and 30% was observed in the glue adhesive. The results showed that the addition of 3 %wt 2MI to FBE caused a decrease in its tensile strength value to 6.63 MPa, and this was better compared to samples 0 and 1. The first, second, and third points during the process were observed at 5.82 MPa, 8.45 MPa, and 5.64 MPa. Figure 10 (d) shows that fracture occurred in 80% of cohesive FBE, and 20% was seen in the glue adhesive. Based on ISO 12944 part 9, the pull-off adhesion test must reach a minimum of 5 MPa [24]. After 2MI is carried out into the FBE, it will improve the coating quality by increasing the adhesion value between the pipe surface and the FBE and fulfilling predetermined criteria.

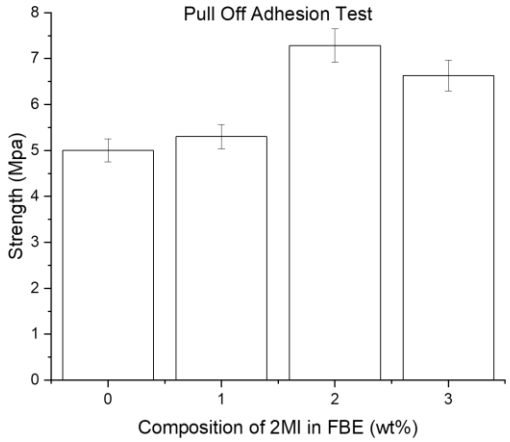

Figure 11. Graph the effect of addition 2MI in FBE strength (adhesion)

The graph in Figure 11 shows that the addition of 2MI increased the adhesion strength value, and the highest composition used was 2 %wt. Furthermore, the tensile strength value of the samples is expected to increase by adding more concentration. This was because the addition of 2MI content to the FBE increased the internal deformation ability, thereby causing a decrease in the cross-linking density. However, the percentage of fracture in samples 0 and 1 has a failure of ≥ 50%, which shows the inconsistent strength of the adhesion on the glue adhesive, resulting in a maximum coating adhesion strength value not being obtained compared to samples 2 and 3 as long as the adhesion strength value reaches a minimum value of 5 MPa. There is no adhesion failure between the pipe surface and the coating, indicating that the coating has good performance and surface preparation.

Porosity and Morphology Analysis

The objective was to determine the porosity formed on the FBE layer, which has been added with 2-methylimidazole. This was because the composition affected the amount of porosity formed. The existence of pores has an impact on the mechanical properties and permeability capabilities of the coating, which correlates with electrochemical testing. To determine the degree of porosity in the coating is determined according to the CSA/CAN Z245.20 standard, as shown in Figure 12. Furthermore, the results of observations are described in Figures 13, Figure 14, Figure 15, and Figure 16 below.

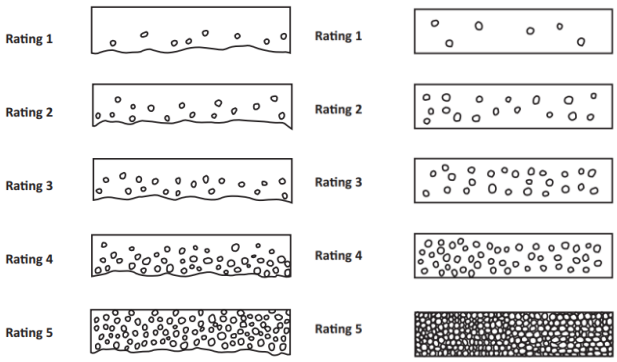

Figure 12. Example of (a) cross-section and (b) interface porosity [12]

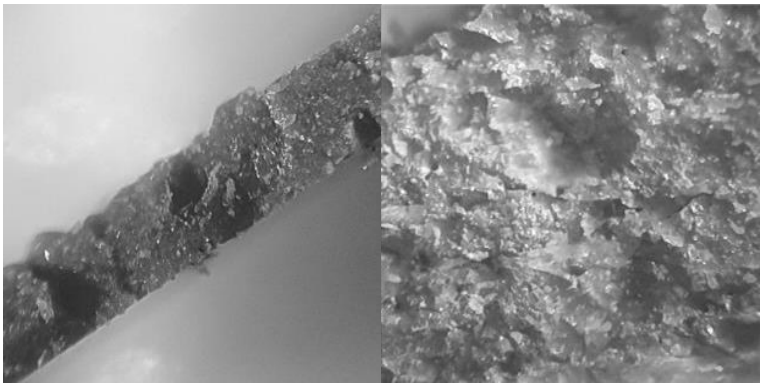

Figure 13. Optical microscope observation with 50× magnification on FBE (a) cross-section and (b) interface

Based on Figure 13, the porosity level in the FBE sample before the addition of 2MI with 50× magnification was at a good level with a rating value of 1 on the cross-section and coating interface section. In the cross-section of the fracture, irregular patterns were formed as part of the coating attached to the surface of the steel pipe due to the roughened steel. This finding indicated that the coating has very good roughness to create a mechanical bond with the steel pipe surface.

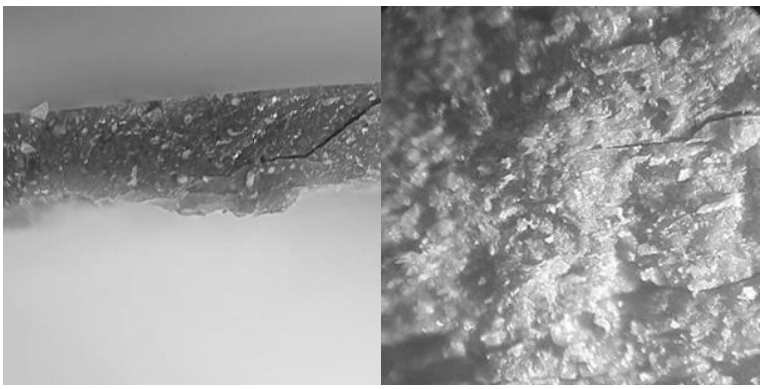

Figure 14. Optical microscope observation with 50× magnification on FBE with 1%wt 2MI (a) cross-section and (b) interface

Figure 14 showed that the porosity rate in the FBE sample with the addition of 1 %wt 2MI with 50× magnification was low. The results showed that the values obtained were in the rate one category for the cross-section and coating interface section. Porosity still occurred, but the addition of 2MI reduced the number of pores, thereby reducing the sample size. The yellow color formed a layer of steel that stuck to the coating. This was due to the sampling technique, which involved bending of the coating to ensure it peels off from the surface of the steel pipe.

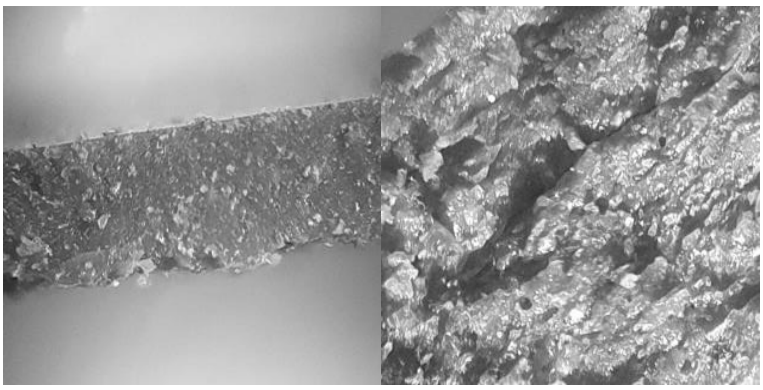

Figure 15. Optical microscope observation with 50× magnification on FBE with 2 %wt 2MI (a) cross-section and (b) interface

Based on Figure 15, the porosity level in the FBE sample with the addition of 2 %wt 2MI with 50× magnification was equal to the initial value with a rating of 1 on the cross-section and coating interface section. However, on observing the interface between the coating and the steel pipe surface, the porosity increased. The results showed that increasing the size of the pores made it easier to load and reduce the level of coating resistance.

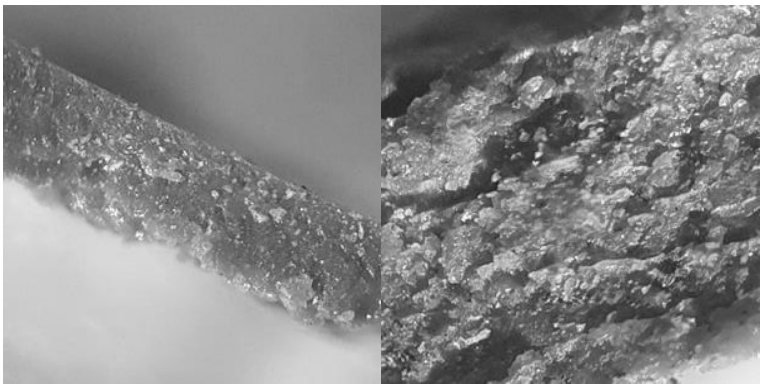

Figure 16. Optical microscope observation with 50× magnification on FBE with 3 %wt 2MI (a) cross-section and (b) interface

In Figure 16, the porosity level in the FBE sample with the addition of 3 %wt 2MI with 50× magnification had a low porosity rating of 1 on the cross-section and coating interface section. Furthermore, porosity was almost invisible on the cross-section and interfacial sections.

The addition of 2MI will reduce the pores size and amount of porosity formed after the application of the coating at low temperatures compared to before the addition because the degree of porosity is strongly influenced by the application temperature used and the curing level of the coating. Lower temperatures will result in an under-cured coating, wherein the coating will reduce its properties and adhesion ability with the pipe surface, resulting in disbonment. 2MI is able to increase the activation energy so that curing at low temperatures can occur and cross-linking density is formed [10]. High cross-linking density will reduce the number and size of the pores formed. This test correlates with the cathodic disbondment test, where low temperature applications produce within a maximum 6.5 mm radius. The test results show that the porosity level formed has a rating of 1 for all samples. Based on the CSA Z245.20, acceptance criteria allowed for porosity levels at rating 1–4, and the addition of 2MI to the coating already meets the requirements [12].

CONCLUSION

The results showed that the addition of 2-methylimidazole (2MI) to fusion bonded epoxy (FBE) has a direct impact on the application temperature. The peak curing temperatures of 1, 2, and 3 %wt were obtained sequentially at 182.90^{o}C, 150.48^{o}C, 140.64^{o}C, and 134.76^{o}C. Differential scanning calorimetry (DSC) experiments revealed that with the introduction of 2MI into the FBE system, the exothermic peak of the FBE system was about 56^{o}C lower than that of the powder manufacture recommendation. Furthermore, there was a shift in the temperature value of the glass, which indicated that the FBE material had experienced a complete curing process. The addition of 2MI also reduced the activation energy and facilitated the curing process. During the mixing of 2MI with FBE, the curing reaction occurred in 2 stages. 2MI served as an anionic polymer in the first phase, where the active hydrogen of the secondary amine in the imidazole was added to the epoxy group. The intramolecular complexes of positive and negative ions can then be formed by generating adducts and other epoxy groups. So that the low temperature application is very good in the application process because the FBE coating has cured perfectly. Meanwhile, the low temperature application process will result in an uncured process and coating failure, such as disbondment/loose adhesion under cathodic conditions. Based on electrochemical characterization analysis using potentiodynamic polarization, the best corrosion rate was obtained after

the addition of 1 %wt 2MI, namely 0.00991 mm/year with a current density of 0.847µA/cm^2. The electrochemical impedance spectroscopy (EIS) method showed that the maximum charge transfer resistance and coating capacitor capacitance after the addition of 1 %wt 2MI was 9.9 kΩ and 8.45×10^{-5} F, respectively. The use of this concentration also produced the widest Nyquist semi-circle width and the largest resistance plot. This shows that the addition of 2MI will increase corrosion resistance compared to before. The cathodic current resistance test was carried out to determine the corrosion resistance of the coating under cathodic condition, and the best result of 4.32 mm was obtained from the addition of 1 %wt 2MI. This test correlates with the EIS test, where the addition of 1 %wt 2MI will increase corrosion resistance due to increased cross-linking density and increased adhesion between the coating and the pipe surface. An increase in the additive concentration can reduce the cross-linking density due to the presence of epoxy-imidazole adducts. Based on mechanical analysis with tensile adhesion testing, adding 2MI increased the maximum tensile strength value at a concentration of 2 %wt 2MI, namely 7.28 MPa, but decreased with further additions. The addition of 2MI did not significantly affect the porosity of the coating with low-temperature applications of 170–175ºC. All samples reached rating 1 in the longitudinal cross-section and the interface between the coating and the steel pipe surface. That indicates that the addition of 2 MI does not reduce the performance of the coating because the increase in density and the size of the porosity do not change in size, inhibiting the ionic transfer process. Therefore, the application of 1 %wt 2MI at low temperatures of 170–175ºC is suitable for coating application on pile pipes with good performance based on predetermined standards, while the high-temperature application is hard to obtain. All failures, such as delamination and cathodic disbondment, can be avoided in low temperature applications.

ACKNOWLEDGEMENT

This study was supported/partially supported by Metallurgical and Materials Engineering of Universitas Indonesia lecturers who provided ideas and suggestions. The authors are grateful to the Coating Laboratory of PT Krakatau Pipe Industries, which provided the facilities for carrying out laboratory testing processes. The authors are also grateful to Corrosion Materials and Metallurgical Engineering Laboratory of Institut Teknologi Sepuluh November and Sentra Teknologi Polimer BPPT, which assisted in technical electrochemical and chemical structure testing.

REFERENCES

[1]. W. D. Callister and D. G. Rethwisch. *Materials Science and Engineering an Introduction (Tenth Edition)*. USA: Johny Willey & Son, Inc, 2018.

[2]. H. Sukanto, W. W. Raharjo, D. Ariawan, J. Triyono, and M. Kaavesina. "*Epoxy resins thermosetting for mechanical engineering*." *Open Engineering*, vol. 11, no. 1, 2021, pp. 797–814.

[3]. E. Aksu. ”Chapter 14–Thermosets for pipeline corrosion protection,” in *Thermosets*, 2nd ed., Q. Guo, Ed. Amsterdam: Elsevier Ltd, 2018, pp. 453–476.

[4]. D. Wong, C. Lam, and P. Singh. “Development of low application temperature coating systems for steel pipelines,” in *Proceedings of the NACE International Corrosion Conference & Expo*, 2018, pp. 1–10.

[5]. A. G. Bannov, A. E. Brester, A. A. Shestakov, M. V. Popov, N. I. Lapekin, and G. K. Krivyakin. “Technological characteristics of epoxy/carbon black composites.” *Materials Today: Proceedings*, vol. 31, no. 3, pp. 496–498, 2020.

[6]. D. Wang, E. Sikora, and B. A. Shaw. “A Study of the effects of filler particles on the degradation mechanisms of powder epoxy novolac coating systems under corrosion and erosion.” *Prog. Org. Coat*, vol. 121, pp. 97–104, 2018.

[7]. E. Licsandru, M. Gaysinski, and A. Mija. “Structural insights of humins/epoxidized linseed oil/ hardener terpolymerization.” *Polymers*, vol. 12, no. 7, 2020.

[8]. Y. R. Ham, S. H Kim, Y. J. Shin, D. H. Lee, M. Yang, J. H. Min, and J. S. Shin. “A comparison of some imidazoles in the curing of epoxy resin.” *J. Ind. Eng. Chem.*, vol. 16, no. 4, pp. 556–559, 2010.

[9]. X. Wan, J. Liu, X. Chen, and J. Wang. “Study on tri-imidazole derivatives modified with triazine-trione structure as latent curing agents for epoxy resin.” *SN Appl. Sci.*, vol. 4, no. 24, 2022.

[10]. J. Xu, J. Yang, X. Liu, H. Wang, J. Zhang, and S. Fu. “Preparation and characterization of fast-curing powder epoxy adhesive at middle temperature.” *R. Soc. open sci.* vol. 5, p. 180566, 2018.

[11]. *Plastics-Differential scanning calorimetry (DSC)-Part 1: General principles*, ISO 11357-2, 2020.

[12]. *Plant-Applied External Coating for Steel Pipe*, CSA 245.20, Canadian Standard Association Group, 2022.

[13]. *Paints and Varnishes—Guidelines for The Determination of Anticorrosive Properties of Organic Coatings by Accelerated Cyclic Electrochemical Technique*, ISO 17463, 2022.

[14]. *Standard Test Method For Pull-Off Strength of Coatings using Portable Adhesion Testers*, ASTM D4541, 2022.

[15]. C Păcurariu, I. Lazău, and R. Lazău. “Kinetic studies of the dehydroxylation and crystallization of raw kaolinite and fluorides-modified kaolinite.” *J Therm Anal Calorim.*, vol. 127, pp. 239–246, 2017.

[16]. E. Benˇova´, V. Zelenˇa´k, D. Halamova´, M. Alma´ˇsi, V. Petrul'Ova´, M. Psotka, and V. Hornebecq. "A drug delivery system based on switchable photo-controlled p-coumaric acid derivatives anchored on mesoporous silica." *J. Mater. Chem. B.*, vol. 5, pp. 817–825, 2017.
[17]. X. Fei, W. Wei, F. Zhao, Y. Zhu, J. Luo, M. Chen, and X. Liu. "Efficient toughening of epoxy–anhydride thermosets with a biobased tannic acid derivative." *ACS Sustainable Chem. Eng.*, vol. 5, no. 1, pp. 596–603, 2017.
[18]. K. Aida, M. Hirao, A. Funabashi, N. Sugimura, E. Ota, J. Yamaguchi. "Catalytic reductive ring opening of epoxides enabled by zirconocene and photoredox catalysis." *Chem.*, vol. 8, no. 6, pp. 1762–1774, 2022.
[19]. C. Feng, Y. Cao, L. Zhu, Z. Yu, G. Gao, Y. Song, H. Ge, and Y. Liu. "Corrosion behavior of reduced-graphene-oxide-modified epoxy coatings on N80 steel in 10.0 wt% NaCl solution." *Int. J. Electrochem. Sci.*, vol. 15, pp. 8265–8276, 2020.
[20]. R. Hermawan. "The Effect of Fly Ash Utilization in Reinforcement Concrete: A Review." *Indonesian Journal of Engineering Science.*, vol. 3, pp. 4, 2022.
[21]. M. Xu, C. N. C. Lam, D. Wong, and E. Asselin. "Evaluation of cathodic disbondment resistance of pipeline coatings–A review." *Progress in Organic Coatings*, vol. 146, p. 105728, 2020.
[22]. M. H. Nazir and Z. A. Khan. "A review of theoretical analysis techniques for cracking and corrosive degradation of film-substrate systems." *Engineering failure analysis*, vol. 72, pp. 80–113.
[23]. J. Wang, J. Hu, C. Gu, Y. Mou, J. Yu, and X. Zhong. "The effect of pulse current cathodic protection on cathodic disbondment of epoxy coatings." *Progress in organic coatings*, vol. 170, p. 107001, 2022.
[24]. *Paints and varnishes — Protective paint systems and laboratory performance test methods for offshore and related structures*, ISO 12944-9, 2018.